IEEE Open Journal of
Power Electronics

Received 11 October 2022; revised 7 November 2022; accepted 14 November 2022. Date of publication 17 November 2022;
date of current version 30 November 2022. The review of this article was arranged by Associate Editor Lingxiao Xue.

Digital Object Identifier 10.1109/OJPEL.2022.3222865

GaN Active Rectifier Diode

MICHAEL BASLER [1] (Graduate Student Member, IEEE), RICHARD REINER [1], STEFAN MOENCH [1] (Member, IEEE), PATRICK WALTEREIT[1], AND RÜDIGER QUAY [1,2] (Senior Member, IEEE)

[1]Fraunhofer Institute for Applied Solid State Physics IAF, 79108 Freiburg, Germany
[2]Department of Sustainable Systems Engineering (INATECH), University of Freiburg, 79108 Freiburg, Germany

CORRESPONDING AUTHOR: MICHAEL BASLER (e-mail: michael.basler@iaf.fraunhofer.de)

This work was supported in part by Fraunhofer Internal Programs under Grant PREPARE 840 229.

ABSTRACT Active or synchronous rectification is used today to further increase the efficiency of mass-market power supplies by eliminating the turn-on voltage of rectifier diodes, thus reducing conduction losses. However, the active rectification is usually realized by two devices: a power MOSFET and a control circuit to imitate an ideal diode behavior. This paper presents a GaN active rectifier diode consisting of a 600 V power transistor, a control circuit with gate driver, and a supply generation, all monolithically realized in a GaN power integrated circuit (IC). This enables a true two-terminal device that can directly replace a rectifier diode. In order to evaluate the proposed conduction loss reduction by replacing a rectifier diode by an active diode, the theoretical limits at circuit level and at semiconductor level are analyzed. The GaN active rectifier diode is demonstrated in a half-wave rectification (110/230 V_{AC}, 50/60 Hz) up to a forward current of 6 A. A single-device realization of low-loss GaN active rectifier diodes is more cost-efficient than a multi-chip or package-integrated solution.

INDEX TERMS Gallium nitride, power integrated circuits, monolithic integrated circuits, active circuits, rectifiers, AC-DC power conversion.

I. INTRODUCTION

Active or synchronous rectification is the replacement of a diode by an active controlled switch to eliminate the turn-on voltage V_{T0} for reducing the conduction losses and increasing energy efficiency. In this context, the term ideal or active diode is often used, which also designates a device with two terminals. One of the most common uses of synchronous rectification is in switched-mode power supplies on the secondary side of the transformer in a variety of different isolated DC-DC converter topologies. Already in the early 70's the effect on efficiency especially at low output voltage levels was investigated [1]. Driven by the efficiency standards of the last 20 years and other factors such as power density, synchronous rectification has become essential in today's power supplies [2]. Over these years, a wide variety of approaches for many topologies have been published, exemplified in [3] as an overview for the LLC resonant converter. But also in AC-DC rectifiers of power supplies, the last percentage points of efficiency are gained by active bridge rectification [4], [5], [6], [7] as cost-effective alternative to bridgeless topologies. However, there are also other applications for active rectification in general, e.g., as battery protection, ORing power supplies and replacement of bypass diodes in photovoltaic modules [8], [9]. Another area of application is in alternator generators for vehicles with internal combustion engines, where the rectification of the three-phase alternating voltage with active diodes can contribute to a saving of 1.2–1.8 g CO_2/km per alternator due to the conduction loss reduction [10], [11].

What all these active rectifier diodes and circuits have in common is that they consist of at least two semiconductor-based components, devices, or dies in different technologies. One component is a power switch, usually silicon (Si) or silicon carbide (SiC) MOSFETs, although gallium nitride (GaN) HEMTs have been increasingly used for synchronous rectification in recent years [3]. Reasons for this are the superior physical properties compared to Si [12], [13] and on the other hand the zero reverse recovery of GaN due to the absence of the body diode [14]. A GaN HEMT with corresponding output characteristic as an active diode is shown in Fig. 1. The other component is the control, which detects the voltage zero crossing in order to imitate an ideal diode behavior. Usually, Si-based bipolar-CMOS-DMOS (BCD) technologies are used

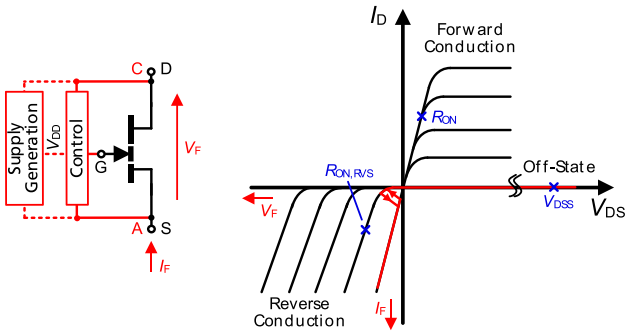

FIGURE 1. Symbol and schematic output characteristic of GaN HEMT modified with a control and optionally a supply generation resulting in a GaN active rectifier diode.

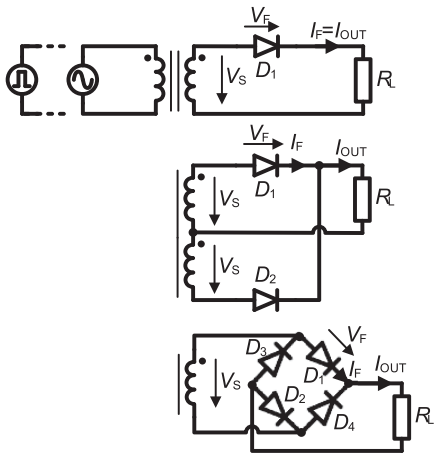

FIGURE 2. Diode rectifier with sine or square wave source and resistive load: (Top) Half-wave rectifier M1U, (middle) full-wave rectifier with center-tapped transformer M2U and (bottom) Full-wave rectifier B2U.

for these ICs [15]. A voltage supply generation is required to provide a two-terminal device and replace conventional diodes directly. There are commercial synchronous rectifier controller ICs for LLC, forward, or flyback converter available from many semiconductor manufacturers [15]. However, there are a few products available for replacing a bridge rectifier to an active bridge using active diodes with breakdown voltages up to 650 V. One approach is to drive four power MOSFETs by using one [7] or two synchronous rectification controller ICs [4], [6] with further additional circuitry. All solutions can directly replace standard bridge rectifiers with 4 connections. Another approach is to replace the rectifier diodes with a single IC each [5], which is realized by a package integration of a power MOSFET and at least one further control IC. However, this approach still requires a power supply for each active or ideal diode with an additional bulk capacitor [5]. Similar approaches with integrated voltage supply for lower breakdown voltages are demonstrated in [10], [16]. In addition, there are numerous patents [17], [18], [19], [20], [21], [22], [23] for active diodes in different voltage classes, which mostly consist of the three parts: power switch, control, and voltage supply generation. A novel approach is to integrate the components of an active diode into the GaN-on-Si technology on a single chip with a low-cost and large-area Si carrier substrate. The lateral structure enables monolithic integration with the power device. The GaN power integration is a technology trend in power electronics [24] and many publications as well as products were presented in this field [12], [24], [25], [26], [27], [28], [29]. There are already commercial HEMTs with package integrated driver and control, which switch on the HEMT in the 3rd quadrant accordingly to a synchronous FET operation and is called "ideal diode mode" [14], [30]. Approaches for battery protection with bi-directional HEMTs are also being pursued [24]. The GaN-based active diode can realize a two-terminal device and enable plug-and-play replacement of conventional rectifier diodes to reduce development time and system cost. The steadily declining costs of the GaN technology could lead to more cost-efficient GaN rectifier diodes in the future and thereby open up a new application area for GaN.

In this article, we present an approach of a GaN active rectifier diode. For this purpose, the theoretical limits are analyzed in terms of circuitry and semiconductor material, which defines a new figure-of-merit (FOM), in Section II. The design of the GaN power IC as active diode is described in detail in Section III based on the three parts: power HEMT, control and voltage supply generation. The experimental results of a first prototype GaN active rectifier diode is shown and compared with the state-of-the-art in Section IV. Section V summarizes the article and discusses the potential of the GaN active rectifier diode.

II. THEORETICAL LIMITS

In this section the theoretical limits of the active diode are discussed in relation to the reduction of the conduction losses, which account for the largest part of the losses of rectifier diodes. At first, investigations are described from a circuit engineering point of view using the rectifier circuits. Afterwards the max. limits of the active diode are described from a physical point of view.

A. CIRCUITRY

This work is limited to the most important single-phase rectifiers: Half-wave rectifier (M1U), full-wave rectifier with center-tapped transformer (M2U) and full-wave rectifier (B2U). The voltage source is decoupled via an ideal transformer with a transmission ratio 1:1, shown in Fig. 2. Once again, there are several loss mechanisms for a conventional diode, e.g., conduction losses, leakage current losses, reverse recovery losses, and also for an active diode, e.g., gate charge losses and losses in the gate driver and control circuits in addition to the previous losses, but here we focus exclusively on the conduction losses. We assume that the active diode switches on ideally, without delay and thus without on and off switching threshold compared to Fig. 1. At the same time, a linear model is applied for the diode and the active diode.

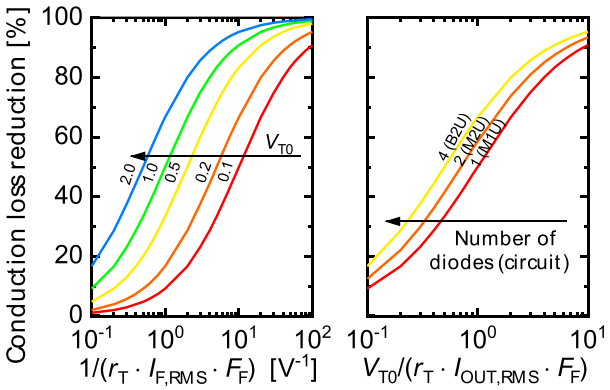

FIGURE 3. Theoretical circuit limits for the replacement of a diode by an active diode. (Left) Conduction loss reduction as a function of the term $1/(r_T \cdot I_{F,RMS} \cdot F_F)$ for one diode with different turn-on voltage from 0.1 to 2.0 V and (right) Depending as a function of the term $V_{T0}/(r_T \cdot I_{OUT,RMS} \cdot F_F)$ for rectifier circuits M1U, M2U, and B2U.

This theoretical circuit analysis investigates the reduction of conduction loss by replacing the diodes with active diodes for the three rectifier circuits M1U, M2U, and B2U. The conduction loss reduction (relation between conduction losses of the active diode $P_{LOSS,AD}$ and diode $P_{LOSS,D}$) can be calculated as

$$\frac{P_{LOSS,AD}}{P_{LOSS,D}} = \frac{R_{ON} \cdot I_{F,RMS}^2}{V_{T0} \cdot I_{F,AV} + r_T \cdot I_{F,RMS}^2}, \tag{1}$$

whereas I_F is the forward current (AV: average, RMS: root mean square), V_{T0} is the turn-on voltage of the diode, r_T is the differential resistance of the diode and R_{ON} the on-resistance of the active diode. It is assumed that $r_T = R_{ON}$ and the following applies $I_{F,AV} = {F_F}^{-1} \cdot I_{F,RMS}$, where F_F is the form factor. The form factor of a halve wave is $\pi/2$ and of a square wave $\sqrt{DC^{-1}}$. DC is the duty-cycle of the square wave. Thus, the formula (1) can be simplified as follows

$$\frac{P_{LOSS,AD}}{P_{LOSS,D}} = \left(1 + \frac{V_{T0}}{F_F \cdot r_T \cdot I_{F,RMS}}\right)^{-1}. \tag{2}$$

Fig. 3 shows the conduction loss reduction in percent depending on the term $1/(r_T \cdot I_{F,RMS} \cdot F_F)$ for one diode with different turn-on voltages from 0.1 to 2.0 V. A rectification with sine wave and diode parameter $V_{T0} = 1$ V, $r_T = 100$ mΩ, $I_{F,RMS} = 6.37$ A results in $1/(r_T \cdot I_{F,RMS} \cdot F_F) = 1$. If this diode would be replaced by an active diode with the same on-resistance, a reduction in conduction loss of 50% results. This example shows the enormous potential of active rectification. Fig. 3 also shows the conduction loss reduction depending on the term $V_{T0}/(r_T \cdot I_{OUT,RMS} \cdot F_F)$ for the rectifier circuits M1U, M2U and B2U. For M1U is valid $I_{OUT,RMS} = I_{F,RMS}$, for M2U $I_{OUT,RMS} = \sqrt{2} \cdot I_{F,RMS}$, and for B2U $I_{OUT,RMS} = 2 \cdot I_{F,RMS}$. If the load (see Fig. 2) is capacitively filtered, the form factor is of course $> \pi/2$, due to the current peaks and the non-sinusoidal shape of, for example, a mains rectification. An analysis was performed in [31].

B. PHYSICAL

The physical limits of the active diode are investigated compared to conventional Schottky rectifier diode. As a basis for a material comparison for unipolar power devices, the ideal specific on-resistance or area-specific on-resistance is calculated as a function of the breakdown voltage for 3-dimensional channel structure. The breakdown voltage V_{BD} can be calculated via the triangular electric field distribution with the max. critical electric field strength E_C. The result is

$$R_{ON} \cdot A_{3D} = \frac{4}{\varepsilon \cdot \mu \cdot E_C^3} V_{BD}^2 [32], \tag{3}$$

where μ is the carrier mobility and ε is the permittivity. The denominator is known as Baliga's figure-of-merit (BFOM). However, the lateral heterojunction of the GaN HEMT is realized with a 2-dimensional channel. In [33], the 2-dimensional theoretical limit of the on-resistance is analyzed using a slanted field plate with a rectangular field distribution. This result is

$$R_{ON} \cdot A_{2D} = \frac{2\sqrt{2}}{\varepsilon \cdot \mu \cdot E_C^3} V_{BD}^2. \tag{4}$$

The formula (3) and (4) only describe the drift zone of the power device for a 2- (for GaN HEMT) or 3-dimensional channel structure. Thus, the drift resistance is the specific on-resistance: $R_{DRIFT} = R_{ON} \cdot A_{2D/3D}$. The forward voltage V_F of a Schottky diode has two contributions, the turn-on voltage of the Schottky metal contact and channel resistance due to drift and substrate region. The forward voltage is given by

$$V_{F,D} = \phi_B + \frac{kT}{q} \ln\left(\frac{J_F}{A^* \cdot T^2}\right) + (R_{DRIFT} + R_{SUB}) \cdot J_F [32], \tag{5}$$

whereas Φ_B is the Schottky barrier height, J_F is the forward current density, $A*$ is the Richardson's constant, T is the temperature and R_{SUB} is the substrate resistance. However, if the active diode is assumed, only the influence of the drift resistance occurs for the forward voltage, which is given by

$$V_{F,AD} = R_{DRIFT} \cdot J_F. \tag{6}$$

Fig. 4 shows the forward voltage calculated by formula (5) and (6) with the physical material properties for Si, SiC and GaN from [32], [34] and a forward current density of 100 A/cm^2. It shows that for low breakdown voltages the drift resistance has a very small influence on the diode or Schottky diode. At higher breakdown voltages with the corresponding material, however, this part dominates. The theoretical limits are based only on forward and breakdown voltage of unipolar devices. However, the switching characteristic is important especially for fast switching applications, which is shown in the FOM of the product of on-resistance and gate charge ($R_{ON}.Q_G$) as a function of the breakdown voltage V_{BD} [35]. Due to the low reverse recovery charge of SiC Schottky diodes, they are preferred for fast-switching applications, while PiN rectifier diodes are used for rectification of the mains voltage. PiN diodes, however, are bipolar devices for

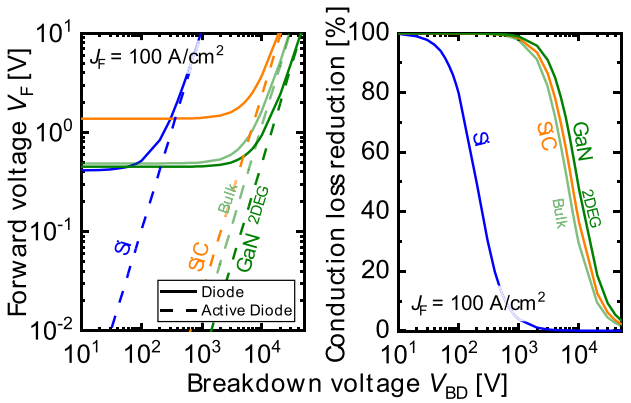

FIGURE 4. Theoretical physical limits for the replacement of a diode by an active diode: (Left) Forward voltage as a function of the breakdown voltage for a diode and active diode and (right) Conduction loss reduction as a function of the breakdown voltage. Both for the material Si, SiC as well as GaN (2-dim. and 3-dim.) and the forward current density of 100 A/cm² scaled to the area.

which the theoretical limits in Fig. 4 do not apply. Fig. 4 also shows the conduction loss reduction as a function of the breakdown voltage for the same forward current density scaled to the area. The conduction loss reduction is calculated from the ratio of $V_{F,AD}/V_{F,D}$, which is proportional to the ratio of the conduction loss. It can be seen that the conduction reduction decreases with increasing breakdown voltage. For SiC and GaN, the percentage reduction over a larger breakdown voltage range is higher than for Si. It should be mentioned that these are the maximum ideal limits of these materials related to the chip area. However, conduction losses are not the only losses of the diode or active diode.

III. GAN POWER IC DESIGN

This section presents the design of the monolithic integrated GaN active rectifier diode in a p-GaN power IC platform. The platform with building blocks is presented in [36]. A first hybrid design was published in [37]. The active diode consists of the three parts: power switch, control and voltage supply generation, which are shown in Fig. 5. The target application of the design is to replace rectifier diodes in mains application at 110/230 V_{AC} and 50/60 Hz. The mode of operation is explained in detail in Section III-B. Fig. 5 also shows the circuit schematic with the external components (R_{SENSE}, R_3, R_5, R_6, C_1, C_2, C_3). These are realized externally for flexibility during testing, but can also be integrated. The GaN power IC has a chip area of 3×2.5 mm². The area of the control and supply generation is only 36.7% while the power device is 63.3% of the chip area.

A. POWER HEMT

In order to have a certain safety margin in mains applications, the power HEMT belongs to the 600 V-class. With a very high gate width >100 mm, a high current carrying capacity is provided. Fig. 1 shows the GaN power HEMT with its output characteristic. The HEMT is operated in the 3rd quadrant: $I_F = I_S$ and $V_F = V_{SD}$. Usually, the threshold voltage of an e-mode HEMT is between 1-2.5 V. If the HEMT is turned off, $V_{T0} = V_{GS} - V_{TH}$ is valid in the third quadrant or reverse conduction [38]. At $V_{GS} = 0$ V, the HEMT behaves like a diode or also called lateral field-effect rectifier (LFER) in the reverse conduction. The slope in the off-state is lower than in the on-state ($R_{ON,RVS} > R_{ON}$, see Fig. 1). The active diode is first in the off-state (e.g., $V_{GS} = 0$ V) and then changes to the on-state (e.g., $V_{GS} = 5$ V) or vice versa. The voltage drop in reverse conduction is 2-3 times higher for the GaN HEMT than that of the MOSFET's body diode [3], [14]. To further reduce conduction losses, an Schottky barrier diode (SBD) can be integrated in parallel with the HEMT as a free-wheeling diode (FWD). This results in a lower turn-on voltage V_{T0} and a reduced on-resistance in the 3rd quadrant. A FWD can be integrated in an area-efficient way [35], [38]. However, the high voltage drop in revere conduction of a HEMT without FWD can also be used advantageously for the voltage supply generation.

B. CONTROL

In general, the control of the active diode consists of a gate driver and a unit for detecting the turn-on and -off point. The gate driver (in Fig. 5: Q_6-Q_9, D_2, C_1) ensures fast turn-on and turn-off switching. GaN-based gate drivers have already been described in many publications [39], [40], [41], [42], [43], [44], [45], [46], [47], [48], [49], [50], [51], [52]. There are several approaches to realize the control unit, e.g., by detecting the voltage polarity with [16], [21] and without current mirror [19], [23], or by detecting the current with current mirror and transimpedance amplifier [18]. An advantage of an additional current mirror is the reduction of the reverse or blocking voltage at the input of the detecting unit. Therefore, control units with current mirror are more suitable for active high-voltage diodes used in mains application [5], [20].

The standard detection method is the voltage detection. The anode voltage V_A is compared with the cathode voltage V_C in an operational amplifier, comparator or hysteresis comparator. Often the anode voltage is additionally increased by a reference voltage [17], [22], [23], [53], [54]. In the SmartRectifier product portfolio from Infineon/ International Rectifier, a hysteresis comparator is used to have two thresholds V_{TH1} and V_{TH2} for turn-on and -off switching of the active diode. Another operational amplifier is needed for a third threshold voltage. Additional control logic has been incorporated a min. on and off time to prevent false turn-off. The threshold voltages are in the range between 0-23 mV (V_{TH1}), 50–263 mV (V_{TH2}), and −2.5–5.4 V (V_{TH3}) [53], [54].

A rather uncommon method is the current detection with sense transistor (SenseFET) in an active diode [18]. With the SenseFET approach, the current through the main transistor Q_1 results in a proportional current through the sense or mirror transistor Q_2 if the intrinsic behavior of the transistors are

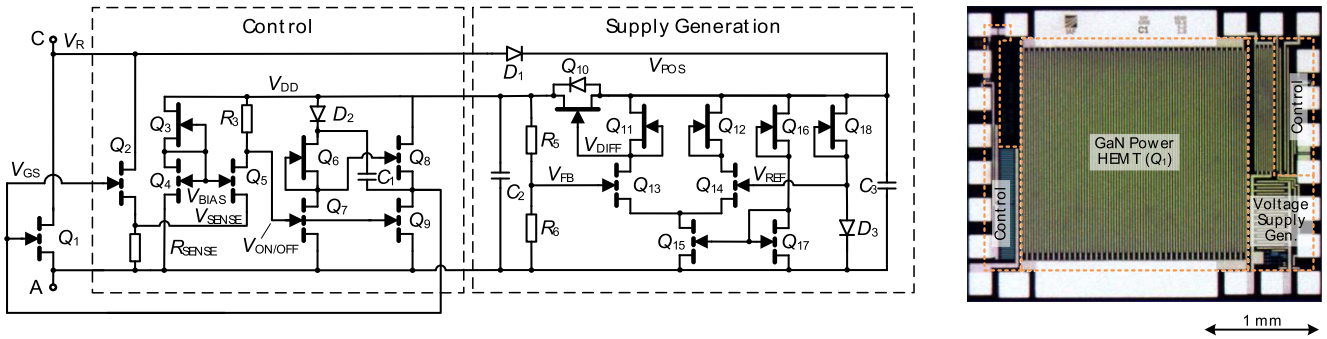

FIGURE 5. **The GaN active rectifier diode realized in a p-GaN power IC platform for active rectification with the three parts: power HEMT, control, and voltage supply generation. (Left) Circuit schematic also with the external components R_{SENSE}, R_3, R_5, R_6, C_1, C_2, C_3 and (right) Chip photo with a total chip area of 3×2.5 mm².**

similar. This current mirror ratio k is defined as

$$k = \frac{I_{D,Q2}}{I_{D,Q1}} = \frac{W_{G,Q2}}{W_{G,Q1}} = \frac{R_{ON,Q1}}{R_{ON,Q2}}, \tag{7}$$

whereas I_D is the drain current, W_G is the gate width and R_{ON} is the on-resistance. The SenseFET approach is also called SenseGaN using GaN [55]. A transimpedance amplifier is connected to the sense transistor which converts the current into a voltage. This amplifier requires a negative voltage supply. Also known in this context as virtual ground sensing [56]. The current threshold can be adjusted with an additional reference voltage. The output signal is usually further analog processed before it controls the gate driver.

Another novel approach of this work (Fig. 5) is the combination of current and voltage detection. Similar to [16], the current is detected by a sense transistor Q_2 and an additional sense resistor R_{SENSE}. The voltage drop V_{SENSE} across the resistor is given by

$$V_{SENSE} = I_{D,Q1} \cdot R_{ON,Q1} \cdot \frac{R_{SENSE}}{R_{SENSE} + R_{ON,Q2}} \text{ [37]}$$

$$= -I_F \cdot R_{ON,Q1} \,|_{k \ll 1,\quad R_{SENSE} \gg R_{ON,Q2}}. \tag{8}$$

For the ratio between the on-resistance of the main and mirror transistor $k = R_{ON,Q1}/R_{ON,Q2} \leq 1/100$ should apply and the sense resistor should be highly resistive, e.g., 10 kΩ, which already described in a work of the author [37]. With this dimensioning, Q_2 has only a small influence on the sense path. Following the input network, the voltage V_{SENSE} is amplified by a common-gate circuit. Fig. 6 shows the output characteristic of the common-gate stage. With the bias voltage, the curve can be shifted to the left or right. It should apply $V_{BIAS} \leq V_{TH,Q5}$, where $V_{TH,Q5}$ is the threshold voltage of the transistor Q_5 in the common-gate stage in Fig. 5. The bias voltage V_{BIAS} can be provided by a voltage divider or a current mirror (as in Fig. 5 realized by Q_3 and Q_4) and for the current mirror, this results in $V_{BIAS} = V_{TH,Q4}$. The threshold voltage of e-mode HEMTs with same voltage class should be nearly equal and homogeneous in a GaN power IC platform, therefore $V_{TH,Q4} = V_{TH,Q5}$ applies. $V_{BIAS} > V_{TH}$ is very critical, because this adjustment can lead to a permanent

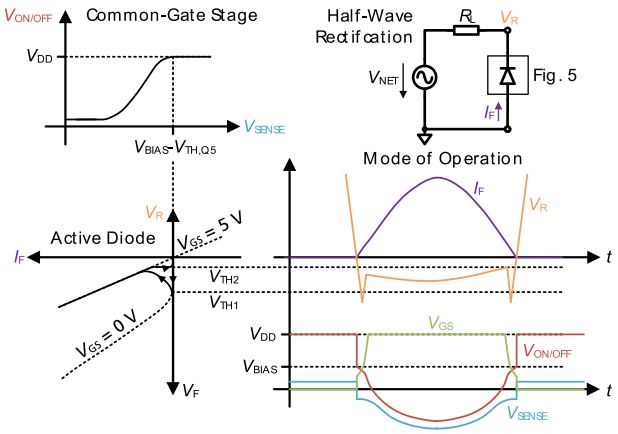

FIGURE 6. **(Left) Output characteristic of the common-gate stage and active diode and (right) Mode of operation in a half-wave rectification with sinusoidal input voltage V_{NET} of the GaN active rectifier diode, which is shown in Fig. 5.**

turn-on of the main transistor. The gain applies to the max. gradient in the output characteristic curve. The lack of p-type devices lead to a low single stage gain of about 10 V/V in GaN [57]. Fig. 6 also shows the mode of operation in a half-wave rectification with sinusoidal input voltage V_{NET} and resistive load R_L of the GaN active rectifier diode, which is shown in Fig. 5. The two threshold voltages V_{TH1} and V_{TH2} are plotted in the time diagram and projected into the output characteristic with hysteresis of the active diode. The hysteresis is caused external positive feedback of the control to Q_1/Q_2 and requires no internal positive feedback as in the case of voltage detection with hysteresis comparator. The output signal of the common-gate stage $V_{ON/OFF}$ must also be inverted to control the active diode correctly. A gate driver stage is used additionally to ensure a fast switching of the main transistor Q_1. With a higher value of R_3 or V_{BIAS} an earlier turn-on or later turn-off of the active diode can be achieved by reducing the threshold voltages. The advantage compared to other concepts is the simplicity of the common-gate stage, which causes hysteresis without complex high-gain amplifiers such as operational amplifiers or comparators. The input network consisting of

a sense transistor and resistor also enables the use in mains applications, which was also presented (not monolithically integrated) by the author in [37] and a patent application was filed by the author in [58]. The author's novel approach combines the advantages of voltage and current detection with a simple readout circuit.

C. VOLTAGE SUPPLY GENERATION

An internal voltage supply generation is required to realize a true two-terminal active diode. There are two possibilities for providing a supply voltage. One possibility is to take the energy for the supply voltage in the conducting phase and the other possibility is to take it in the blocking phase. Both options have advantages and disadvantages and can be realized by conventional concepts such as charge pumps, linear regulators or Zener diodes. A disadvantage of the generation in the conducting phase is that the voltage drop over the active diode is very small <1–4 V. In addition, the supply must be able to block the complete reverse voltage of the active diode. There is an approach that uses the input network of sense transistor and resistor of the control and then increases the voltage V_{SENSE} by a charge pump to the desired supply voltage. The supply voltage would be available after a certain time [16]. This possibility is very complex due to the low voltage ($V_{SENSE} < V_F$). However, an additional half-wave rectification is necessary in the blocking phase consisting. The challenge with generation in the blocking phase is that the supply voltage should be available in the complete conduction phase and must therefore, be stored. The voltage range is very high in the blocking phase and conventional concepts such as Zener diode or linear regulator can be used to realize a stable supply voltage. Fig. 5 exemplary shows a design of a voltage supply generation for the blocking phase. This design is particularly suitable for mains applications. The configuration consists of half-wave rectification and high-voltage linear regulator, which generates the supply voltage. The half-wave rectification is implemented by a high-voltage diode D_1. The rectified voltage V_{POS} have to be stored by at least one capacitor, because the supply voltage must be guaranteed in the conducting phase of the active diode. The size of the input capacitor C_3 is strongly dependent on the current consumption of the control, but can also be operated without. The input voltage V_{IN} of the linear regulator corresponds V_{POS}, while the output voltage V_{OUT} is equal to V_{DD}. Fig. 5 shows a completely novel type of linear regulator. As usual, this linear regulator also consists of a pass element Q_{10}, a feedback network R_5/R_6 and an error amplifier Q_{11}-Q_{15}. The error amplifier in this case is a differential amplifier with current source loads. It compares the feedback voltage V_{FB} with a reference voltage V_{REF}. The diode-based reference voltage is realized by a current source Q_{18} and a diode D_3. A feature of this linear regulator is that the pass element is a d-mode transistor. This avoids the need for a charge pump with n-type transistors for a higher overdrive or low dropout. In addition, the transistor Q_{10} has an integrated free-wheeling diode [35], which is required for the conditions where V_{POS} is less than V_{DD}.

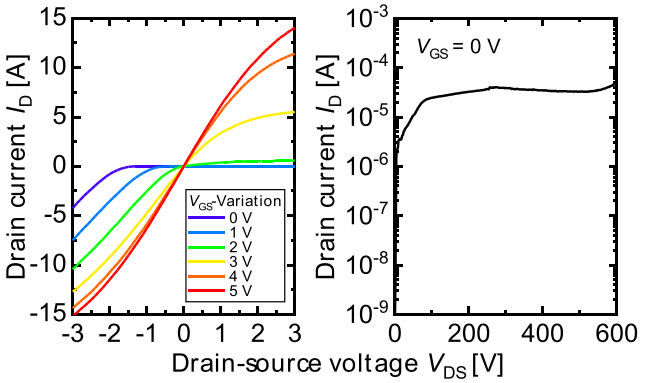

FIGURE 7. Static measurements of the main transistor Q_1 of the two samples. (Left) Output characteristic with V_{GS} = 0–5 V/1 V. (Right) Breakdown characteristic at V_{GS} = 0 V.

IV. EXPERIMENTAL RESULTS AND DISCUSSION

The IC shown in Fig. 5 was processed and fabricated in two different multi-project wafer runs but with the same layout.

Fig. 7 shows static measurements of the main transistor Q_1. The IV characteristic shows six curves with gate-source voltages V_{GS} from 0 to 5 V. The on-resistance is 161 mΩ at $|V_{DS}| = 1$ V, $V_{GS} = 5$ V. The 2DEG sheet resistance has a value of 1108 Ω/□. The transistor Q_1 requires an area of 4.75 mm^2, which result in a $R_{ON}.A$ of 7.65 mΩcm^2 or a forward voltage of 0.765 V scaled with a forward current density of 100 A/cm^2. The off-state (drain) leakage current is 38.3 μA at $V_{DS} = 300$ V, $V_{GS} = 0$ V. The threshold voltage is 1.6 V. With GaN technology optimization, the on-resistance can be further reduced to values <161 mΩ.

In the next step, the GaN active rectifier diode is characterized in a half-wave rectification in a mains application (110/230 V_{AC}, 60/50 Hz) with a resistive load R_L up to a forward current of 6 A, as shown in Fig. 6. For this purpose, another device with a higher on-resistance of 320 mΩ but similar process parameters was taken from a second GaN technology process run. Fig. 8 shows the time signals for the half-wave rectification. The supply voltage V_{DD} of 5 V is realized externally. The supply current is ∼0.7 mA (in standby) and ∼3 mA (in switching operation). The supply current can be decreased by reducing the current through D_2, Q_6, and Q_7. This in turn slows down the turn-on and -off transition. V_{SENSE} changes the polarity at voltage zero crossing. This voltage is amplified by the common-gate stage and then inverted by the bootstrapped NOT gate. The bias voltage V_{BIAS} is 1.5 V. The turn-on and turn-off point is not symmetrical and shows a kind of hysteresis behavior. The turn-on delay of the control is ∼6.2 µs and the turn-off delay is ∼0.2 µs. The reverse voltage V_R was additionally measured using a clamping circuit (clipper clp1500V15A1), which has a non-linear behavior and saturation at $V_R \approx 1.8$ V. With higher temperature, the on-resistance increases, similar to commercial GaN HEMTs or power ICs, and thus the forward voltage increases.

Fig. 9 shows the results as IV curve of the GaN active rectifier diode as combination of static and transient measurements

TABLE 1. Comparison of Different Active Diodes

Parameters	SM74611 [9]	AOZ7270DI [5]	LMG342xR030 [30]	Y. Kagawa et al. ISPSD'2009 [16]	Y. Senzaki et al. PCIM'2020 [10]	This work
Kind of active diode	Bypass diode	Rectifier diode	HEMT with driver[1]	Rectifier diode	Rectifier diode	Rectifier diode
Device Rating	30 V/15 A	600 V/20 A	600 V/40 A	200 V/~50 A	>15 V/~100 A	600 V/15 A
Realization	Package	Package	Package	Multiple Packages	Package	IC (monolithic)
Power device	MOSFET	MOSFET	HEMT	2× MOSFETs	MOSFET, Z-Diode	HEMT
Control component	Control IC	Min. 1× control IC	Control IC	Control IC	Control IC	Int. control (mono.)
Switching frequency	-	50-60 Hz	Max. 2.2 MHz	60 Hz	800 Hz	>1000 Hz
Switching thresholds	-	-105 mV (ON), 1 mV (OFF)	0 V/0 A (ON/OFF)	~300 mV (ON), ~100 mV (OFF)	~600 mV (ON)	~300 mV (ON), ~100 mV (OFF)
Delay times	~3 ms (ON, max. on-time ~100 ms)	For 50 Hz sinusoidal	50 ns (ON), 50 ns (OFF)	~1 ms (ON), ~0.5 ms (OFF)	~50 ns (ON)	~6.2 µs (ON), ~0.2 µs (OFF)
Two-Terminal Device	Yes	No	No	Yes	Yes	Yes
Kind of supply. gen.	Charge pump (Conducting phase)	-	-	Charge pump (Conducting phase)	Half-wave rec. (Blocking phase)	Half-wave rec. with HV linear regulator (Blocking phase)
Supply voltage	-	16 V	7.5-18 V	-	-	5 V
Supply current	-	5-12 µA	0-220 mA	-	-	~3 mA
Add. int. components	Bulk capacitor	-	-	-	Bulk capacitor	(monolithic)

(1) Can be used as active rectifier diode due to the "ideal diode mode" of the integrated driver

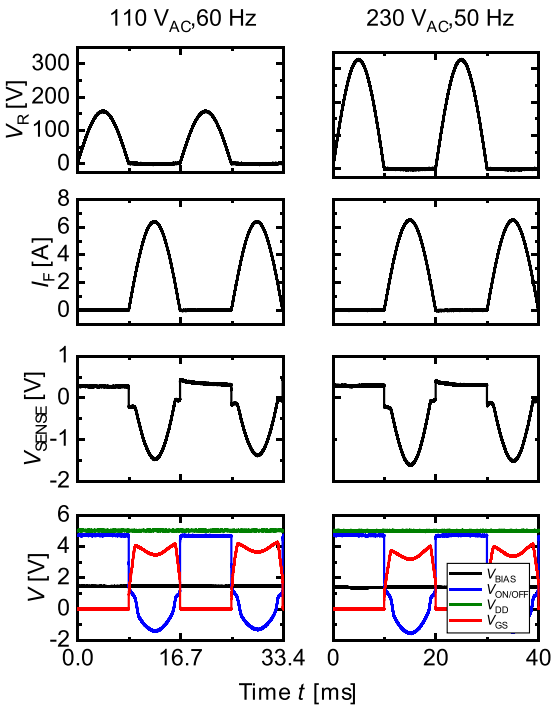

FIGURE 8. Transient measurements of the reverse voltage V_R, forward current I_F and the voltages V_{SENSE}, V_{BIAS}, $V_{ON/OFF}$, V_{DD} and V_{GS} in a half-wave rectification. (Left) 110 V_{AC}, 60 Hz. (Right) 230 V_{AC}, 50 Hz.

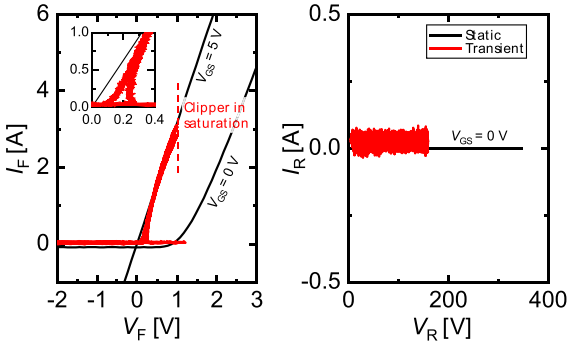

FIGURE 9. IV curve of the GaN active rectifier diode as combination of static and transient measurements at 110 V_{AC}. (Left) Forward characteristic with inset. (Right) Reverse characteristic.

at 110 V_{AC} (Fig. 8, left) between 0–16.7 ms and demonstrates the function of the novel device approach. Both forward and reverse characteristic are shown. The turn-on/-off threshold voltages of the active diode circuit are unsymmetrical as described above and result in ~0.3 V and ~0.1 V, respectively (as shown in the inset of Fig. 9 (left)). By a different dimensioning of the gate circuit these threshold voltages can be further optimized. In detail, the threshold voltages (shown in Fig. 6) can be shifted closer to 0 V by either reducing the bias voltage or the resistance of the common-gate stage. The turn-on voltage of the active diode is already lower than the turn-on voltage of the diode at $V_{GS} = 0$ V starting from a forward current of ~100 mA. At $I_F = 1$ A, the forward voltage of the active diode is 75% lower than that of the LFER. The forward voltage decreases further with increasing current and is proportional to the losses of the diodes. In addition to the forward voltage reduction, rectification is possible in spite of a failure of the voltage supply generation.

Table 1 shows a comparison of different active diodes. Only the active diodes [5], [16], [30] are suitable for rectifying the mains voltage, whereby [30] was developed for fast-switching applications with "ideal diode mode". In all approaches some kind of package integration is aimed, at except in this work, which achieved to monolithically integrate all components of the active diode. This can also have advantages in terms of power density. The delay times of this work is in the µs-range enabling low voltage switching thresholds, which in turn allow a high switching frequency in the range of >1 kHz beyond the 50 Hz application demonstrated in this work. At higher switching frequencies, the abcence of the body diode and the associated zero reverve recovery of the GaN active rectifier diode is a significant benefit. The supply current measured in this work can be further reduced by minimizing the additional power of the supply generation and optimized dimensioning of the logic, sensing, and driver circuit. Thus, the performance

of the GaN active rectifier diode can be further improved in the future, making this concept of monolithic integration in GaN even more attractive in terms of cost, efficiency and performance. The approach can also be combined with other new GaN-based device concepts, e.g., the dual-gate GaN monolithic bidirectional switch with self-reverse-blocking behavior [59] by replacing the low-voltage Si Schottky diode.

V. CONCLUSION

In this work, a GaN active rectifier diode is presented. For this purpose, the theoretical limitations for rectifier diodes from the circuit point of view for M1U, M2U, and B2U, as well as physical limitations when replacing the diode with an active diode, but only with regard to the reduction of conduction loss, are analyzed. The advantages of an active diode and the aspiration of an GaN active diode are thus clarified. The design of the components power switch, control and voltage generation of the active diode with reference to the realization in the GaN-on-Si technology are explained. The manufactured GaN active rectifier diode as GaN power IC requires only 36.6% of the chip area for control and supply voltage generation while the power switch is realized on the remaining chip area. The control consists of a combination of current and voltage detection by a sense transistor and a subsequent amplifier stage. This simple concept allows monolithic integration and hysteresis with two threshold voltages for turn-on and -off. The GaN active rectifier diode is measured in a half-wave rectification at 110/230 V_{AC}, 60/50 Hz with an appropriate resistive load to demonstrate forward currents up to 6 A. The delay times until the HEMT is turned on/off are in the µs-range, resulting in a turn-on/-off threshold voltage of ∼0.3 V and ∼0.1 V, respectively. The GaN active rectifier diodes can directly replace rectifier diodes by the two-terminal realization and be more cost-effective than package-integrated active diodes in the future.

ACKNOWLEDGMENT

The authors would like to thanks the colleagues from the Fraunhofer IAF Epitaxy and Technology Department for their contributions during wafer growth, IC processing, and characterization. The author thanks Dirk Meder for bonding/packaging the test ICs.

REFERENCES

[1] E. R. Pasciutti, "Efficiency/reliability design requirements at low output voltage levels," in *Proc. IEEE Power Electron. Specialists Conf.*, 1971, pp. 13–20.

[2] Y. Développement, "Status of the Power Electronics Industry," *Market Technol. Rep.*, 2019. [Online]. Available: www.yolegroup.com

[3] Y. Wei, Q. Luo, and H. A. Mantooth, "Synchronous rectification for LLC resonant converter: An overview," *IEEE Trans. Power Electron.*, vol. 36, no. 6, pp. 7264–7280, Jun. 2021, doi: 10.1109/TPEL.2020.3040603.

[4] Infineon, "Application note AN_1905_PL52_1905_101502: Design of active bridge line rectification for SMPS," Apr. 24, 2020. Accessed: Dec. 20, 2021. [Online]. Available: https://www.infineon.com/dgdl/Infineon-MOSFET_CoolMOS_S7_600V_active_bridge_SMPS-ApplicationNotes-v01_00-EN.pdf?fileId=5546d46271bf4f92017217bdb69a3a12

[5] Alpha & Omega Semiconductor, "Zero bridge loss' AlphaZBL™ ideal diode," AOZ7270DI: 600V, Sep. 2020. Accessed: Aug. 31, 2021. [Online]. Available: http://www.aosmd.com/res/data_sheets/AOZ7270DI.pdf

[6] Y. Miwa, H. Shoji, J. Sakano, T. Utsumi, and T. Higchi, "Self-powered synchronous rectifying active bridge compatible with diode bridge for commercial rectification," in *Proc. PCIM Europe; Int. Exhib. Conf. Power Electron., Intell. Motion, Renewable Energy Energy Manage.*, 2022, pp. 1–10.

[7] NXP, "TEA2208T: Active bridge rectifier controller," Apr. 14, 2021. Accessed: May 19, 2022. [Online]. Available: https://www.infineon.com/dgdl/ir11672aspbf.pdf?fileId=5546d462533600a4015355c4555 61653

[8] Texas Instruments, "Basics of ideal diodes (Rev. B)," Feb. 2021. [Online]. Available: https://www.ti.com/lit/an/slvae57b/slvae57b.pdf?ts=1659619038131

[9] Texas Instruments, "SM74611 smart bypass diode datasheet (Rev. B)," May 2016. [Online]. Available: https://www.ti.com/lit/ds/symlink/sm74611.pdf?ts=1659685743204&ref_url=https%253A%252F%252Fwww.google.com%252F

[10] Y. Senzaki et al., "Super low loss diode (SLLD) for automotive alternator generators," in *Proc. PCIM Europe Digit. Days; Int. Exhib. Conf. Power Electron., Intell. Motion, Renewable Energy Energy Manage.*, 2020, pp. 1–5.

[11] Infineon Technologies AG, "New ultra-low loss diode for light vehicle generators reduces CO2 emissions - Infineon Technologies," Aug. 10, 2021. Accessed: Aug. 5, 2022. [Online]. Available: https://www.infineon.com/cms/en/about-infineon/press/market-news/2021/INFATV202108-090.html

[12] H. Amano et al., "The 2018 GaN power electronics roadmap," *J. Phys. D: Appl. Phys.*, vol. 51, no. 16, 2018, Art. no. 163001, doi: 10.1088/1361-6463/aaaf9d.

[13] K. J. Chen et al., "GaN-on-Si power technology: Devices and applications," *IEEE Trans. Electron. Devices*, vol. 64, no. 3, pp. 779–795, Mar. 2017, doi: 10.1109/TED.2017.2657579.

[14] Y. Zhang and F. Yang, "Maximizing the performance of GaN with ideal diode mode: Application report," Oct. 2020. Accessed: Sep. 28, 2021. [Online]. Available: https://www.ti.com/lit/an/snoa932/snoa932.pdf?ts=1632735153587&ref_url=https%253A%252F%252Fwww.google.com%252F

[15] Y. Développement, "Power management IC: Technology, industry and trends," *Market Technol. Rep.*, 2019. [Online]. Available: www.yolegroup.com

[16] Y. Kagawa et al., "Low-loss rectifier by self-driven MOSFET with gate drive voltage control circuit," in *Proc. 21st Int. Symp. Power Semicond. Devices IC's*, 2009, pp. 69–72.

[17] A. R. Ball, "Synchronous rectifier and method of operation," U.S. Patent 6,271,712, Aug. 7, 2001.

[18] G. Deboy, "Circuit for an active diode and method for operating an active diode," U.S. Patent 9,577,629, Jun. 4, 2009.

[19] G. Deboy and L. Goergens, "Active diode," U.S. Patent 8031498B2, Oct. 4, 2011.

[20] J. L. Heath and T. W. Barcelo, "Self-biasing ideal diode circuit," U.S. Patent 10333425B1, Jun. 25, 2019.

[21] J.-T. Hwang, S.-O. J. H.-I. Shin, and J. Rhee, "Active diode driver," U.S. Patent 9419608B2, Aug. 16, 2016.

[22] M. Lenz, G. Damiano, P. Ioannis, and P. Albino, "Diodenschaltung," U.S. Patent DE102019104691A1, Aug. 27, 2020.

[23] R.-K. Oswald, T. Yamamoto, T. Ryu, and H. Shirokoshi, "Active diode," U.S. Patent 7199636B2, Apr. 3, 2007.

[24] Y. Développement, "Power GaN 2022," *Market Technol. Rep.* 2022. [Online]. Available: www.yolegroup.com

[25] A. Lidow, "The path forward for GaN power devices," in *Proc. IEEE Workshop Wide Bandgap Power Devices Appl. Asia*, 2020, pp. 1–3.

[26] K. J. Chen et al., "Planar GaN power integration – the world is flat," in *Proc. IEEE Int. Electron. Devices Meeting*, 2020, pp. 27.1.1–27.1.4.

[27] M. Kaufmann and B. Wicht, "A monolithic GaN-IC with integrated control loop for 400-V offline buck operation achieving 95.6% peak efficiency," *IEEE J. Solid-State Circuits*, vol. 55, no. 12, pp. 3169–3178, Dec. 2020, doi: 10.1109/JSSC.2020.3018404.

[28] O. Trescases, S. K. Murray, W. L. Jiang, and M. S. Zaman, "GaN power ICs: Reviewing strengths, Gaps, and future directions," in *Proc. IEEE Int. Electron Devices Meeting*, 2020, pp. 27.4.1–27.4.4.

[29] R. Sun, J. Lai, W. Chen, and B. Zhang, "GaN power integration for high frequency and high efficiency power applications: A review," *IEEE Access*, vol. 8, pp. 15529–15542, 2020, doi: 10.1109/ACCESS.2020.2967027.
[30] Texas Instruments, "LMG342xR030 600-V 30-mΩ GaN FET with integrated driver, protection, and temperature reporting datasheet (Rev. D)," Mar. 2022. [Online]. Available: https://www.ti.com/lit/ds/symlink/lmg3422r030.pdf?ts=1661342663822&ref_url=https%253A%252F%252Fwww.ti.com%252Fproduct%252FLMG3422R030
[31] J. O. Guerra-Pulido, "In-depth analysis of the capacitive filtered half wave rectifier," *Comput. Appl. Eng. Educ.*, vol. 27, no. 1, pp. 236–248, 2019, doi: 10.1002/cae.22071.
[32] B. J. Baliga, *Gallium Nitride and Silicon Carbide Power Devices*. Singapore: World Scientific, 2017.
[33] W. Saito, I. Omura, T. Ogura, and H. Ohashi, "Theoretical limit estimation of lateral wide band-gap semiconductor power-switching device," *Solid-State Electron.*, vol. 48, no. 9, pp. 1555–1562, 2004, doi: 10.1016/j.sse.2003.10.003.
[34] U. K. Mishra, L. Shen, T. E. Kazior, and Y. -F. Wu, "GaN-based RF power devices and amplifiers," *Proc. IEEE*, vol. 96, no. 2, pp. 287–305, Feb. 2008, doi: 10.1109/JPROC.2007.911060.
[35] R. Reiner et al., "Integrated reverse-diodes for GaN-HEMT structures," in *Proc. IEEE 27th Int. Symp. Power Semicond. Devices IC's*, 2015, pp. 45–48.
[36] M. Basler et al., "Building blocks for GaN power integration," *IEEE Access*, vol. 9, pp. 163122–163137, 2021, doi: 10.1109/ACCESS.2021.3132667.
[37] M. Basler et al., "A GaN-based active diode circuit for low-loss rectification," in *Proc. 33rd Int. Symp. Power Semicond. Devices ICs*, 2021, pp. 59–62.
[38] R. Reiner, P. Waltereit, B. Weiss, R. Quay, and O. Ambacher, "Investigation of GaN-HEMTs in reverse conduction," in *Proc. PCIM Europe, Int. Exhib. Conf. Power Electron., Intell. Motion, Renewable Energy Energy Manage.*, 2017, pp. 1–8.
[39] H. Xu, G. Tang, J. Wei, Z. Zheng, and K. J. Chen, "Monolithic integration of gate driver and protection modules with *P*-GaN gate power HEMTs," *IEEE Trans. Ind. Electron.*, vol. 69, no. 7, pp. 6784–6793, Jul. 2022, doi: 10.1109/TIE.2021.3102387.
[40] Y.-Y. Kao et al., "Fully integrated GaN-on-silicon gate driver and GaN switch with temperature-compensated fast turn-on technique for achieving switching frequency of 50 MHz and slew rate of 118.3 V/Ns," *IEEE J. Solid-State Circuits*, vol. 56, no. 12, pp. 3619–3627, Dec. 2021, doi: 10.1109/JSSC.2021.3103875.
[41] M. Kaufmann, A. Seidel, and B. Wicht, "Long, short, monolithic-the gate loop challenge for GaN drivers: Invited paper," in *Proc. IEEE Custom Integr. Circuits Conf.*, 2020, pp. 1–5.
[42] S. K. Murray et al., "Transient overvoltage detection technique for GaN HEMTs integrated in a 200-V GaN-on-SOI process," in *Proc. IEEE Appl. Power Electron. Conf. Expo.*, 2022, pp. 1400–1405.
[43] Y. Yamashita, S. Stoffels, N. Posthuma, S. Decoutere, and K. Kobayashi, "Monolithically integrated E-mode GaN-on-SOI gate driver with power GaN-HEMT for MHz-Switching," in *Proc. IEEE 6th Workshop Wide Bandgap Power Devices Appl.*, 2018, pp. 231–236.
[44] S. Moench et al., "A 600V p-GaN Gate HEMT with intrinsic freewheeling Schottky-Diode in a GaN power IC with bootstrapped driver and sensors," in *Proc. 32nd Int. Symp. Power Semicond. Devices ICs*, 2020, pp. 254–257.
[45] Navitas Semiconductor, "Application note AN015: New GaNFast™ power ICs with GaNSense™ technology loss-less current sensing & autonomous protection," Dec. 20, 2021. Accessed: Jan. 07, 2022. [Online]. Available: http://navitassemi.com/wp-content/uploads/2021/12/AN015-GaNSense-FINAL-12-20-2021.pdf
[46] Y.-Y. Kao et al., "A monolithic GaN-based driver and GaN power HEMT with diode-emulated GaN technique for 50MHz operation and sub-0.2ns deadtime control," in *Proc. IEEE Int. Solid- State Circuits Conf.*, 2022, pp. 228–230.
[47] M. Basler, R. Reiner, S. Moench, P. Waltereit, and R. Quay, "Function blocks of a highly-integrated all-in-GaN power IC for DC-DC conversion," in *Proc. 24th Eur. Conf. Power Electron. Appl. (Europe)*, 2022, pp. 1–9.
[48] D. Bergogne, G. Regis, V. Rat, F. Rothan, J. Delaine, and T. Bouchet, "Integrated GaN ICs, development and performance," in *Proc. 21st Eur. Conf. Power Electron. Appl.*, 2019, pp. 1–8.
[49] F. Udrea et al., "The smart ICeGaN™ platform with sensing and protection functions for both enhanced ease of use and gate reliability," in *Proc. IEEE 34th Int. Symp. Power Semicond. Devices ICs*, 2022, pp. 41–44.
[50] P. Bau et al., "Static and dynamic measurements for GaN integrated switches," in *Proc. PCIM Europe; Int. Exhib. Conf. Power Electron., Intell. Motion, Renewable Energy Energy Manage.*, 2022, pp. 1–8.
[51] S. K. Murray et al., "On-chip dynamic gate-voltage waveform sampling in a 200-V GaN-on-SOI power IC," *IEEE J. Emerg. Sel. Topics Power Electron.*, early access, Mar. 30, 2022, doi: 10.1109/JESTPE.2022.3163646.
[52] W. L. Jiang et al., "Monolithic integration of a 5-MHz GaN half-bridge in a 200-V GaN-on-SOI process: Programmable dv/dt control and floating high-voltage level-shifter," in *Proc. IEEE Appl. Power Electron. Conf. Expo.*, 2021, pp. 728–734.
[53] International Rectifier, "Application note AN-1087: Design of secondary side rectification unsing the IRS1167 SmartRectifier™ control IC," Mar. 2006. Accessed: Aug. 31, 2021. [Online]. Available: https://www.infineon.com/dgdl/Infineon-Synchronous_rectification_IC_SmartRectifier_IR1167-ApplicationNotes-v01_00-EN.pdf?fileId=5546d462533600a4015355959ea21034
[54] International Rectifier. "IR11672AS: Advanced SmartRectifier™ control IC," Nov. 6, 2013. Accessed: Aug. 31, 2021. [Online]. Available: https://www.infineon.com/dgdl/ir11672aspbf.pdf?fileId=5546d462533600a4015355c455561653
[55] M. Biglarbegian and B. Parkhideh, "Characterization of SenseGaN current-mirroring for power GaN with the virtual grounding in a boost converter," in *Proc. IEEE Energy Convers. Congr. Expo.*, 2017, pp. 5915–5919.
[56] On Semiconductor, "Application note AND8093/D: Current sensing power MOSFETs," Mar. 2017. Accessed: Aug. 31, 2021. [Online]. Available: https://www.onsemi.com/pub/Collateral/AND8093-D.PDF
[57] B. Wicht, "Monolithic GaN–Unleashing the potential by integrating power, sensing and control. PwrSoC 2021," Oct. 26, 2021. Accessed: Feb. 18, 2021. [Online]. Available: http://pwrsocevents.com/wp-content/uploads/2021/11/5.1-Bernhard-Wicht-Monolithic-GaN-%E2%80%93-Unleashing-the-Potential-by-Integrating-Power-Sensing-and-Control.pdf
[58] M. Basler, "Aktive diodenschaltung," DE Patent 10 2020 121 630 A1, Aug. 18, 2022.
[59] N. Nain, S. Walser, J. Huber, K. K. Leong, and J. W. Kolar, "Self-reverse-blocking control of dual-gate monolithic bidirectional GaN switch with Quasi-Ohmic on-state characteristic," *IEEE Trans. Power Electron.*, vol. 37, no. 9, pp. 10091–10094, Sep. 2022, doi: 10.1109/TPEL.2022.3163589.

MICHAEL BASLER (Graduate Student Member, IEEE) received the M.Sc. degree in power and microelectronics from Reutlingen University, Reutlingen, Germany, in 2018. He is currently working toward the Ph.D. degree in the Sustainable System Engineering, University of Freiburg, Breisgau, Germany.

Since 2019, he has been a Research Assistant with the Fraunhofer Institute for Applied Solid State Physics IAF, Freiburg, Germany, where he is involved in the development, design and characterization of GaN-based devices, and ICs for power-electronic applications.

RICHARD REINER received the M.Sc. degree in electrical engineering from the Technical University of Berlin, Berlin, Germany, in 2007, and the Dr.-Ing. degree from the Technical University of Freiburg, Breisgau, Germany, in 2017. Between 2007 and 2010, he was a Research Associate with the Hahn-Schickard-Gesellschaft, Institute for Microsystem Technology in Villingen-Schwenningen, where he worked on developing electronic sensor systems.

Since 2010, he has been a Research Associate with the Fraunhofer Institute for Applied Solid State Physics IAF in Freiburg on the development and characterization of GaN-based devices and circuits for power-electronic applications. He is author or coauthor of more than 100 publications.

STEFAN MOENCH (Member, IEEE) received the B.Sc. and M.Sc. degrees in electrical engineering and information technology from the University of Stuttgart, Stuttgart, Germany, in 2011 and 2014, respectively. He was an Academic Research Assistant with the Institute of Robust Power Semiconductor Systems ILH, University of Stuttgart.

He is currently a Researcher of microelectronics with the Fraunhofer Institute for Applied Solid State Physics IAF, Germany. He defended his doctoral thesis in 2021. His research interests include highly-integrated, highly-efficient, and fast-switching GaN-based power electronics for applications, such as electromobility and renewable energy conversion.

PATRICK WALTEREIT received the Ph.D. degree in physics from the Humboldt-University Berlin, Berlin, Germany, in 2001, on growth and characterization of non-polar oriented GaN/AlGaN hetero structures. From 2001 to 2004, he was a Postdoctoral Researcher with the University of California, Santa Barbara, CA, USA, investigating MBE growth for GaN-based electronic and optoelectronic devices. Since 2004, he has been with the Fraunhofer IAF in Freiburg, Germany, working on GaN based high voltage and high frequency devices. He is currently heading Technology Department.

RÜDIGER QUAY (Senior Member, IEEE) received the Diploma in physics from Rheinisch-Westfälische Technische Hochschule, Aachen, Germany, in 1997, and the Ph.D. degree (Hons.) in technical sciences, the second Diploma in economics, and the Venia Legendi (Habilitation) degree in microelectronics from the Technische Universität Wien, Vienna, Austria, in 2001, 2003, and 2009, respectively. In 2001, he joined the Fraunhofer Institute of Applied Solid-State Physics (Fraunhofer IAF), Freiburg im Breisgau, Germany, in various positions. He is currently the executive Director of Fraunhofer IAF. Since 2020, he has been a Fritz-Hüttinger Professor with the Department for Sustainable Systems Engineering (INATECH), Albert-Ludwig University, Freiburg im Breisgau. He has authored or coauthored more than 350 refereed publications, three monographs, and contributions to two further.